Supporting Information

Sugiyama et al. 10.1073/pnas.1304507110

SI Materials and Methods

Sphere Passage. To passage spheres, the culture media was removed and the Matrigel was overlayed with 0.7 mg/mL Liberase Blendzyme 3 (Roche) dissolved in the S21 culture media. Matrigel was then triturated and incubated at 37 °C for 40 min. The released spheres were collected by centrifugation at 956 × *g* for 5 min at 4 °C, mechanically dissociated in culture media by pipetting, and washed five times with S21 culture media. This procedure produced multicellular clusters and did not disperse spheres completely into single cells. Before plating the dissociated cells, 2×10^4 cells of freshly FACS-purified pancreatic mesenchyme were added to dispersed spheres. Mesenchymal cells sustained expression of the marker Sox9 during passage of spheres in our cultures but were not detectably incorporated in spheres.

Time-Lapse Acquisition. The tissue culture plate was placed in the environmental chamber of an inverted microscope (Zeiss AxioObserver Z1) equipped with a motorized stage. Bright-field images were captured every 4 h for a period of 1 wk, using MetaMorph software (Molecular Devices). MetaMorph was also used for the image analysis. Spheres were cultured in S21 culture media at 21% oxygen.

Floxed Gene Deletion. To activate $CreER^{T2}$ in gene deletion experiments, 10 nM 4-hydroxytamoxifen (Sigma) was added (see Figs. S7 and S8 for the schedule). Target gene deletion was assessed by PCR, using both genomic DNA and cDNA.

Adenoviral Vectors. Mouse *Ngn3* cDNA (BC104326) was purchased from Thermo/Open Biosystems. The EcoRV/BamHI fragment was subcloned into the EcoRV site of the Dual-RFP-CCM shuttle vector (Vector Biolabs). Human *NGN3* cDNA (BC074938.2) was purchased from Thermo/Open Biosystems, and a FLAG tag was attached to the N terminus by PCR. The mutant N89D NGN3 allele was made by targeted mutagenesis (1, 2). Each human cDNA was subcloned into the EcoRI site of Dual-RFP-CCM shuttle vector, which has dual CMV promoters to drive expression of both monomeric RFP and the inserts. The adenoviruses were made and purified by Vector Biolabs. Ad-RFP control virus was also purchased from Vector Biolabs. The backbone of the adenoviral vector is type 5 (dE1/E3). For viral infection, spheres were infected at a multiplicity of infection of 200 at 37 °C in suspension (without Matrigel) for 6 h on passage. Spheres were then washed twice with culture medium and embedded in Matrigel.

Immunohistology. Spheres were released from Matrigel by trituration and digestion with 1 mg/mL dispase in culture medium for 90 min and washed five times with medium. The sphere pellet was resuspended with 100 μL Collagen Gel Kit (Nitta Gelatin). In some experiments, spheres were not released from Matrigel. Rather, Matrigel was washed with liquid collagen once and triturated in 300 μL liquid collagen.

Next, the mixture of spheres, Matrigel, and collagen was transferred into a sterile microfuge tube. Liquid collagen with suspended spheres was solidified, according to the manufacturer's instruction, fixed with 4% paraformaldehyde in PBS for 1 h at 4 °C, and cryo-embedded or paraffin-embedded. To detect Nkx6.1, antigen unmasking was performed in low-pH unmasking solution (Vector Laboratories) at 37 °C for 1 h and the M.O.M. kit (Vector Labs) was used as instructed.

For MafA detection, we boiled frozen sections for 15 min in antigen retrieval solution containing 8 mL Tris·HCL (1.0 M at pH 8) and 0.5 mL EDTA (0.5 M at pH 8) in 200 mL water. Tyramide Signal Amplication (Invitrogen) was used. Sections were stained with antibodies against NGN3 (rabbit, 1/2,000; made in our laboratory), Sox9 (rabbit, 1/100; Chemicon), glucagon (guinea pig, 1/500; Linco), anti–C-peptide (rabbit, 1/100; Cell Signaling Technology), carboxypeptidaseA (rabbit, 1/200; MorphoSys/AbD Serotic), Muc1 (hamster, 1/200; Thermo/Neomarkers), Nkx6-1 (DSHB F55A10, 1/00; University of Iowa, Iowa City, IA), insulin (1/400; Sigma), MafA (1/200; Bethyl Laboratories), Somatostatin (1/200; Dako), and pancreatic polypeptide (1/200; Novus).

For staining Prdm16, FVB/NJ mouse gastrointestinal organs were dissected at E15.5, fixed with 4% paraformaldehyde in PBS overnight at 4 °C, and cryo-embedded. Antigen unmasking was performed in a boiling 1× Target Retrieval Solution (Dako) for 15 min. Endogenous biotin was blocked by using a Streptavidin Biotin Blocking kit (Vector Laboratories). Endogenous peroxidase was blocked by incubating for 1 h in 1% H_2O_2/PBS. Sections then were sequentially stained with antibodies that detect Prdm16 (sheep, 1:50, R&D), Ngn3 (mouse F25A1B3, 1:100; DSHB), and E-cadherin (rat ECCD-2, 1/500; Invitrogen). Prdm16 was visualized with a TSA kit (Invitrogen) before incubation with anti-Ngn3 and anti–E-cadherin antibodies. Secondary antibodies were from Jackson ImmunoResearch and Molecular Probes. Samples were mounted with Vectashield containing DAPI (1.5 mg/mL, Vector Laboratories). Microscopic images were obtained using a Leica SP2 AOBS confocal laser scanning microscope.

To count the average number of cells in each sphere, spheres were released from Matrigel by dispase treatment, washed with media, resuspended in 30 μL of Vectashield containing DAPI, and mounted on a Superfrost plus glass slide. Iterative confocal sectioning through multiple focal planes was performed, and the number of $DAPI^+$ nuclei was counted manually ($n = 43$). For measurement of endocrine cell mass, we dissected pancreas at E18.5 and fixed it with 4% paraformaldehyde (PFA) at 4 °C overnight. We analyzed at least 3 different mice per genotype. For each collected pancreas, we collected a minimum of 12 sections (spanning the entire pancreas) at least 100 μm apart. The total cross-sectional area of $hormone^+$ cells (insulin, glucagon, somatostatin, or pancreatic polypeptide) was added and normalized to total pancreatic area using Image-Pro Plus analysis software (Media Cybernetics). Statistical analysis was performed using a two-tailed Student *t* test. Results were considered significant when $P < 0.05$. α-cell proliferation level was assessed by scoring the number of $Ki67^+$ $glucagon^+$ cells and was expressed as a percentage of the total number of $glucagon^+$ cells counted. For each experiment, at least three mice per genotype were scored, with a minimum of 30 islets per mouse. To measure the average size of $glucagon^+$ cells, $glucagon^+$ cell area was divided by the number of $glucagon^+$ $DAPI^+$ nuclei.

Transmission Electron Microscopy. Samples were fixed in Karnovsky's fixative: 2% glutaraldehyde (EMS) and 4% formaldehyde (EMS) in 0.1 M sodium dacodylate (EMS) at pH 7.4 for 1 h at room temperature. The samples were then cut, postfixed in 1% osmium tetroxide (EMS) for 2 h at 4 °C, washed three times with ultrafiltered water, and *en bloc* stained in uranyl acetate at 4 °C overnight. The samples were dehydrated in a series of ethanol washes for 15 min each at 4 °C, beginning at 50%, 70%, and then 95%, where the samples are allowed to be equilibrated to room temperature. Thereafter, the alcohol was changed to 100% two

times and then replaced with propylene oxide (PO) for 15 min. The samples were infiltrated with EMbed-812 resin (EMS) mixed 1:1 with PO for 2 h followed by two parts EMbed-812–1 part PO overnight. The samples were then placed into EMbed-812 for 2–4 h and placed into molds with fresh resin and placed into a 65 °C oven overnight. Sections were taken between 75 and 90 nm, picked up on formvar/carbon-coated 75 mesh Cu grids and stained for 20 seconds in 1:1 saturated UrAcetate (~7.7%) in acetone, followed by staining in 0.2% lead citrate for 3–4 min. The stained sections were observed with a JEOL 1230 transmission electron microscopy at 80 kV, and photos were taken by a Gatan Multiscan 791 digital camera.

ELISA. For measurement of C-peptide content, spheres were released from Matrigel by trituration and digested with 1 mg/mL dispase in S5 medium for 90 min and washed with medium five times. The spheres were further digested with TrypLE at 37 °C for 5 min. MIP-GFP+ cells were FACS-purified as described earlier. MIP-GFP+ cells were resuspended with 10 mM Tris·HCl, 1 mM EDTA, and 0.1% (wt/vol) BSA at pH 7.0 and sonicated. An aliquot of 2 volumes of acid ethanol (75% vol/vol ethanol, 2% vol/vol concentrated HCl, 23% vol/vol H_2O) was added to MIP-GFP$^+$ and sphere extracts overnight at 4 °C. This extract mixture was used for C-peptide2 ELISA (Alpco Diagnostics). To normalize C-peptide levels, DNA was quantified with Picogreen (Invitrogen). As a comparison we also sorted MIP-GFP$^+$ cells from E17.5 pancreas. Pancreata were digested with 0.05% Trypsin-EDTA (Invitrogen) diluted in PBS at 37 °C for 8 min. The pancreata were triturated for 25 times and spun down, the supernatant was removed, and the pellet was resuspended with a FACS buffer containing EGTA (3), filtered through a 70 μm filter (BD), and FACS sorted as described earlier. For insulin secretion assays, spheres were embedded in Matrigel were washed three times for 20 min each with modified Krebs-Ringer bicarbonate buffer (118 mM NaCl, 2.5 mM $CaCl_2$, 1.2 mM KH_2PO_4, 4.8 mM KCl, 25.3 mM $NaHCO_3$, 1.2 mM $MgSO_4$, 10 mM Hepes, and 0.1% wt/vol BSA at pH 7.4) containing 3 mM glucose. After extensive washing, spheres were incubated consecutively in the indicated low and high levels of glucose or KCl Krebs-Ringer bicarbonate buffer for 1 h. Insulin level was measured with a mouse insulin ELISA kit (ALPCO Diagnostics), as previously described (4).

Quantitative RT-PCR. Total RNA was isolated using the Qiagen RNeasy Micro Kit. cDNA was generated using the Ambion RetroScript Kit. RT-PCR studies were performed using a real-time PCR system from Applied Biosystems. Replicate samples were processed independently, and each cDNA was tested in duplicate. Expression levels were normalized to beta-actin, and then depending on the assay, results were shown as relative levels to whole E11.5 pancreas or littermate controls (Fig. 3) and expressed as the mean ± SEM. In Fig. 3*H*, relative mRNA levels of *Arx* and *Pax4* at E15.5 were measured after eliminating exocrine acinar, mesenchymal, and blood cells in each single pancreas by FACS using CD49f^{low} Ter119^{neg} CD45^{neg} as markers, as described previously (3). Information about primers and probe sets are described in Dataset S5.

1. Jensen JN, Rosenberg LC, Hecksher-Sorensen J, Serup P (2007) Mutant neurogenin-3 in congenital malabsorptive diarrhea. *N Engl J Med* 356(17):1781–1782.
2. Wang S, et al. (2008) Myt1 and Ngn3 form a feed-forward expression loop to promote endocrine islet cell differentiation. *Dev Biol* 317(2):531–540.
3. Sugiyama T, Rodriguez RT, McLean GW, Kim SK (2007) Conserved markers of fetal pancreatic epithelium permit prospective isolation of islet progenitor cells by FACS. *Proc Natl Acad Sci USA* 104(1):175–180.
4. Chen H, Carlson EC, Pellet L, Moritz JT, Epstein PN (2001) Overexpression of metallothionein in pancreatic beta-cells reduces streptozotocin-induced DNA damage and diabetes. *Diabetes* 50(9):2040–2046.

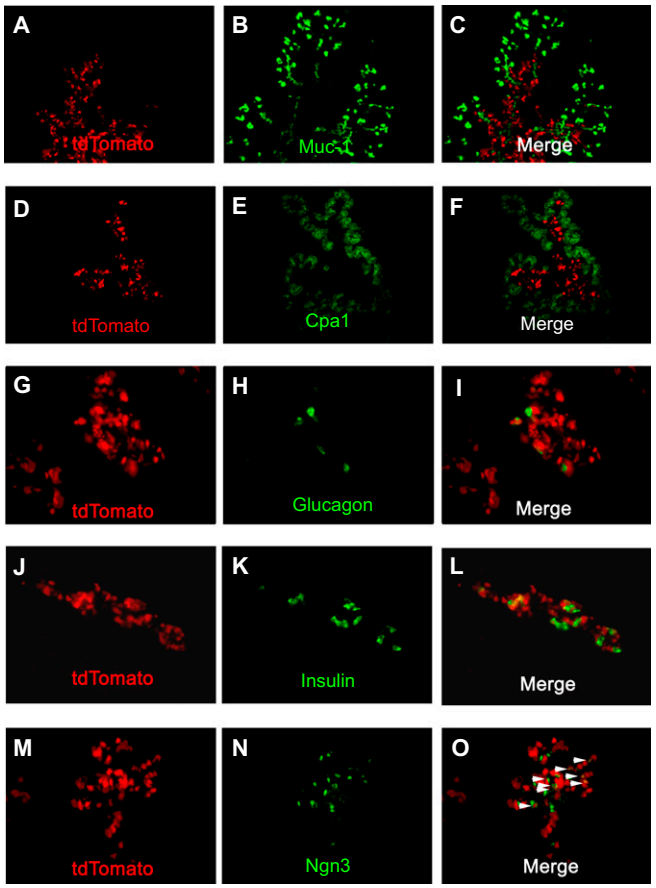

Fig. S1. Immunohistology of E15.5 pancreas from *Ngn3*-tdTomato mice. Cryosectioned tissues were stained with antibodies against Muc1 (*B*), Cpa1 (*E*), glucagon (*H*), insulin (*K*), and Ngn3 (*N*). Panels *A*, *D*, *G*, *J*, and *M* show restricted expression of tdTomato. Panels *C*, *F*, *I*, *L*, and *O* represent merged images. Arrowheads indicate cells coexpressing tdTomato and Ngn3. *Ngn3*-tdTomato specifically labels the fetal pancreatic endocrine lineage.

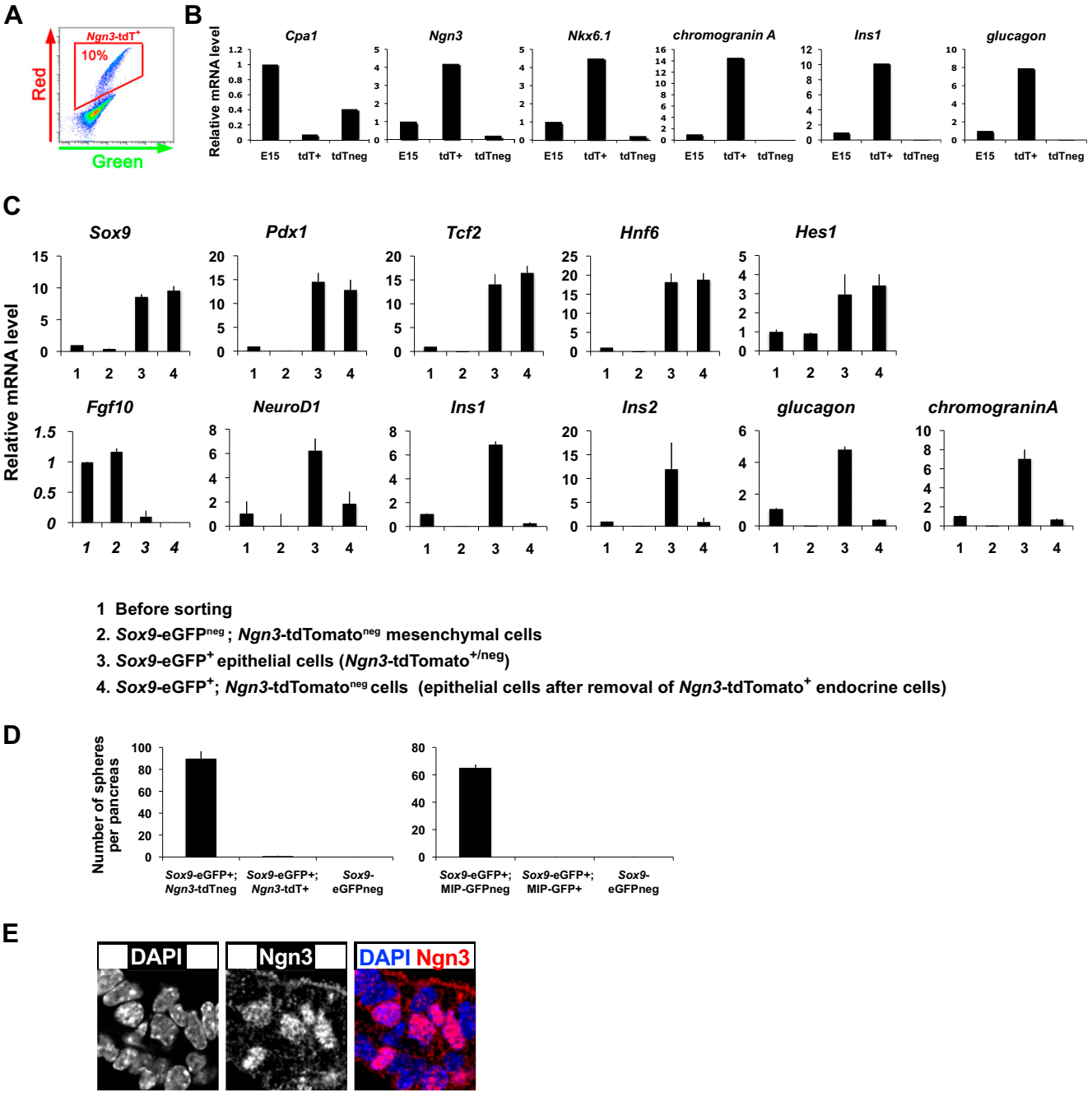

Fig. S2. (*A* and *B*) *Ngn3*-tdTomato lineage-traces endocrine cells at E15.5. (*A*) FACS analysis showing tdTomato-positive (10%) and tdTomato-negative (90%) populations. X axis shows autofluorescence in the green channel. (*B*) Quantitative RT-PCR analysis of the designated genes in unsorted E15 pancreatic cells (E15) and sorted *Ngn3*-tdT^{+} and *Ngn3*-tdT^{neg} cells. (*C*) *Sox9*-eGFP^{+}; *Ngn3*-tdTomato^{neg} cells are enriched for progenitor markers at E11.5. Quantitative RT-PCR analysis of the designated genes in cells separated by FACS from *Sox9*-eGFP; *Ngn3*-tdT pancreas. (*D*) The number of spheres generated from each distinct cell population separated by FACS. (*E*) Immunohistology of pancreatic spheres.

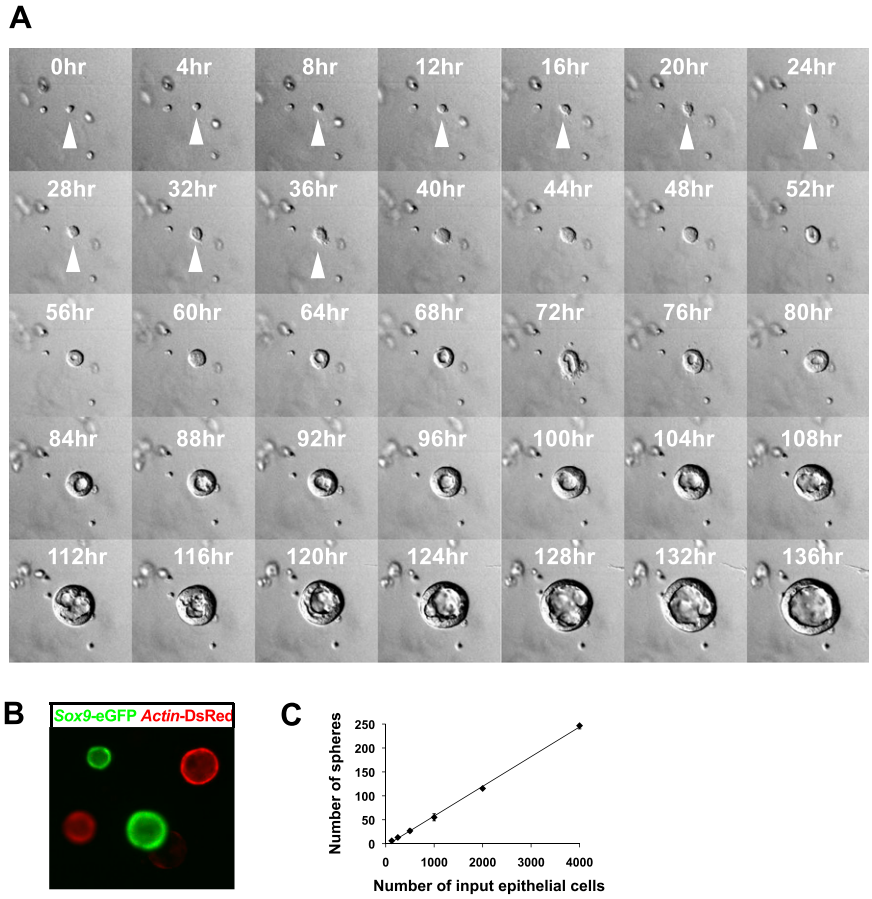

Fig. S3. Sphere growth by proliferation was monoclonal and not achieved by cell migration or aggregation. (*A*) Stills from video-microscopy show a single progenitor cell generating a pancreatic sphere. Arrowheads mark a sphere-forming progenitor cell. (*B*) Clonal assay. Dispersed cells from *Sox9*-eGFP pancreas were mixed with those from *Actin*-DsRed pancreas. Mesenchymal cells were labeled with *Actin*-DsRed and were not detectably incorporated in spheres but were observed in different focal planes outside spheres. (*C*) Limiting dilution analysis, showing linear-correlation between input cells and sphere numbers.

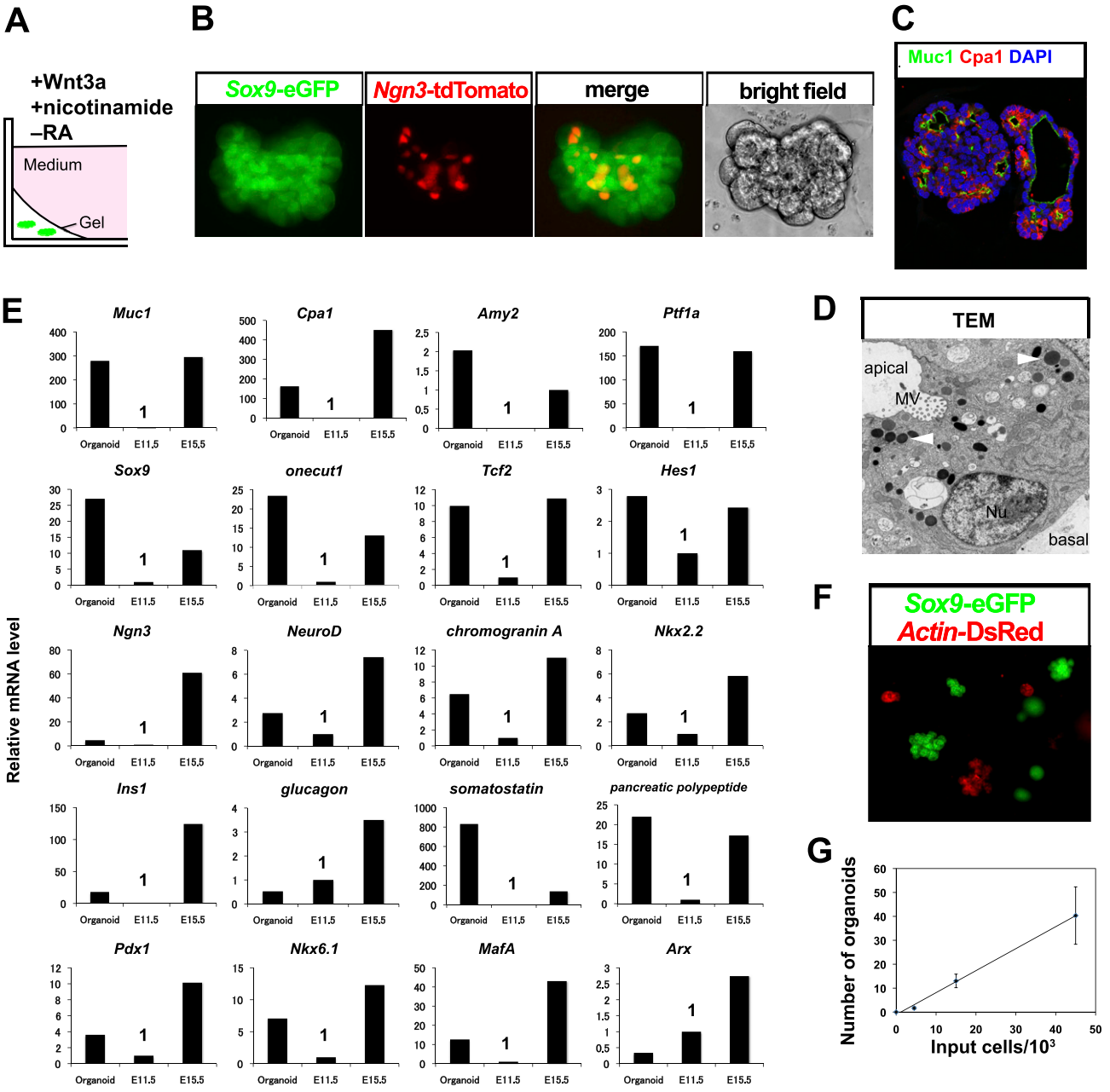

Fig. S4. Reconstitution of monoclonal organoids harboring the principal pancreatic cell lineages. (*A*) Schematic summarizing organoid culture methods. (*B*) Microscopic images showing organoid morphology with cells expressing *Sox9*-eGFP and the endocrine reporter *Ngn3*-tdTomato. (*C*) Immunohistology of organoids stained with anti-Muc1 (green) and anti-Cpa1 (red) antibodies. (*D*) Transmission electron micrograph of organoids. MV, microvilli; Nu, nucleus. Arrowheads: immature zymogen granules. (*E*) Quantitative RT-PCR analysis for expression of the indicated markers in organoids compared with whole E11.5 and E15.5 fetal pancreas. (*F*) Clonal assay: dispersed cells from *Sox9*-eGFP pancreas were mixed with those from *Actin*-DsRed pancreas. (*G*) Linear correlation between the number of organoids and that of input cells. (*C*–*F*) Canonical Wnt signaling agonist R-spondin1 was used instead of Wnt3a. R-spondin1 and Wnt3a generated similar results, although R-spondin1 was slightly more potent than Wnt3a.

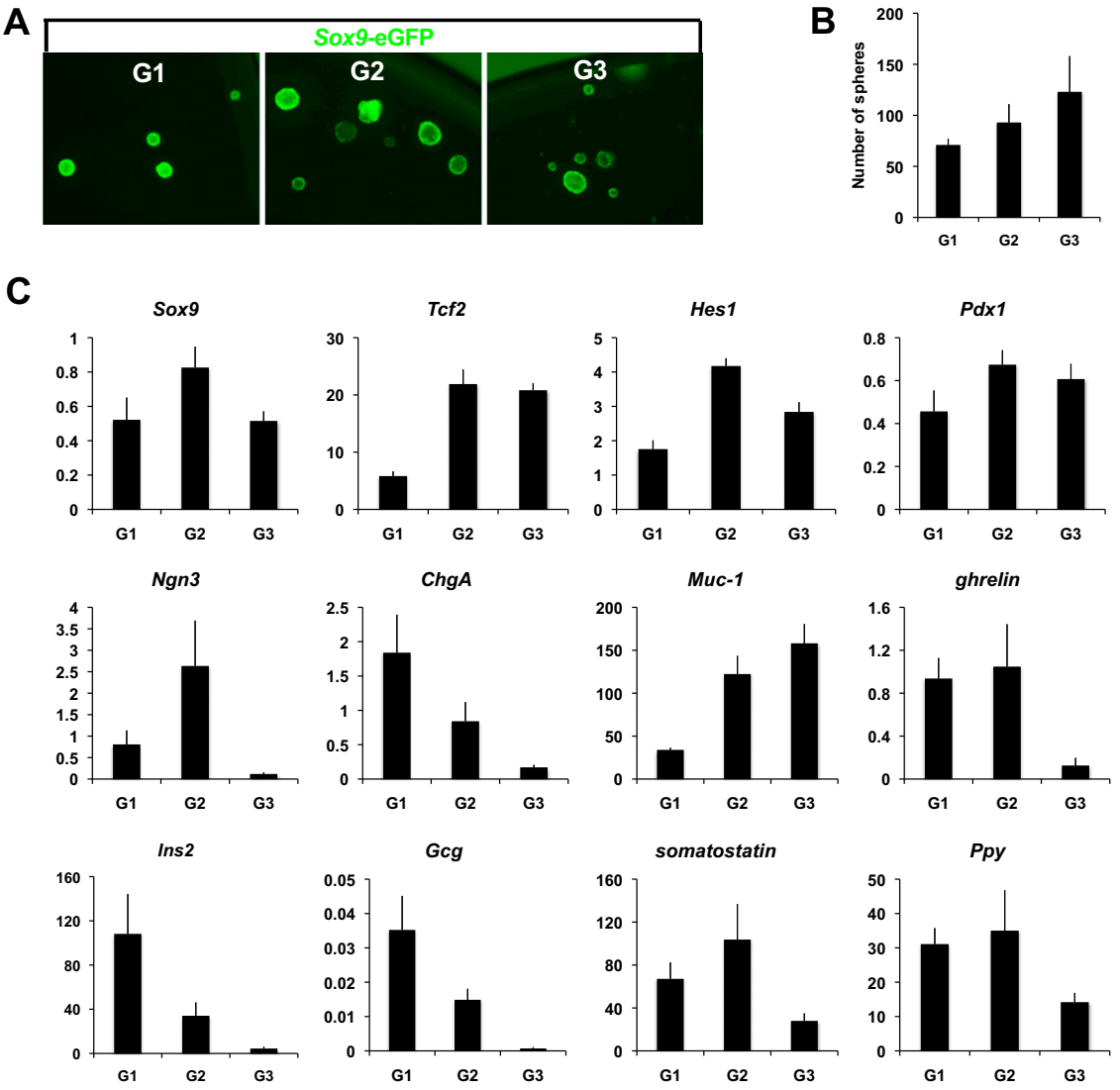

Fig. S5. A reduction in the potential to generate multiple pancreatic cell types during serial passage. (*A*) Maintenance of *Sox9*-eGFP expression through passage of spheres to G3. (*B*) Quantification of sphere number per pancreas after each passage. (*C*) Quantitative RT-PCR analysis of the pancreatic genes ($n = 3$ in each time).

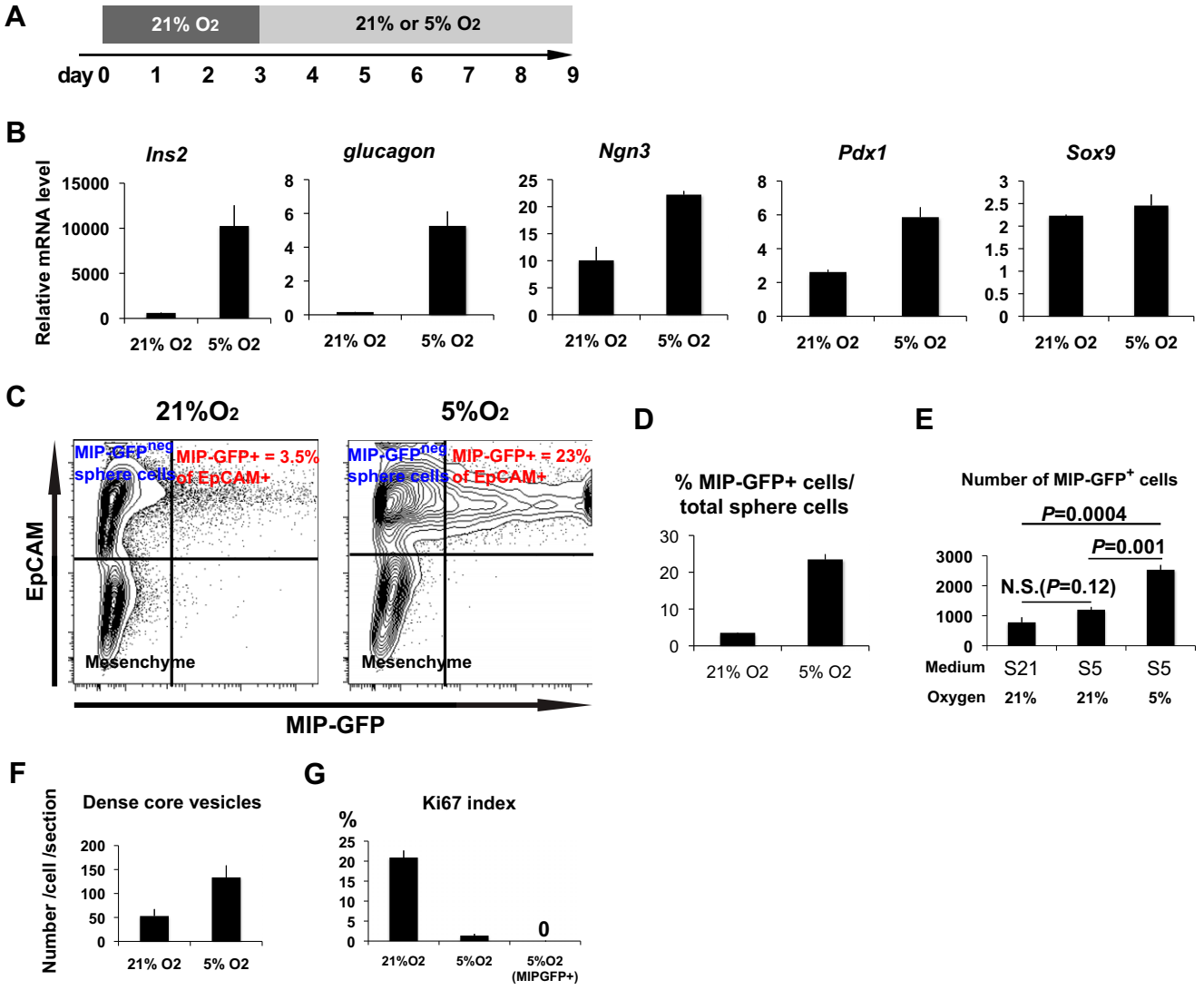

Fig. S6. Physiological oxygen promotes β-cell differentiation. (*A*) Schematic showing the time course of the experiment. (*B*) Quantitative RT-PCR analysis of spheres generated from FACS-purified MIP-GFP^{neg} cells ($n = 3$). (*C*) FACS analysis of cells expressing MIP-GFP and EpCAM in spheres developed in 21% or 5% oxygen. (*D*) Fraction of MIP-GFP^{+} cells in total sphere cells measured by FACS. (*E*) The number of MIP-GFP^{+} cells in each indicated condition quantified by FACS. (*F*) Quantification of DCVs per cell per electronmicrographic section ($n = 3$–5). (*G*) Ki67 index measured by immunohistology. Ki67 staining was not detected in sphere MIP-GFP^{+} cells cultured in physiological oxygen.

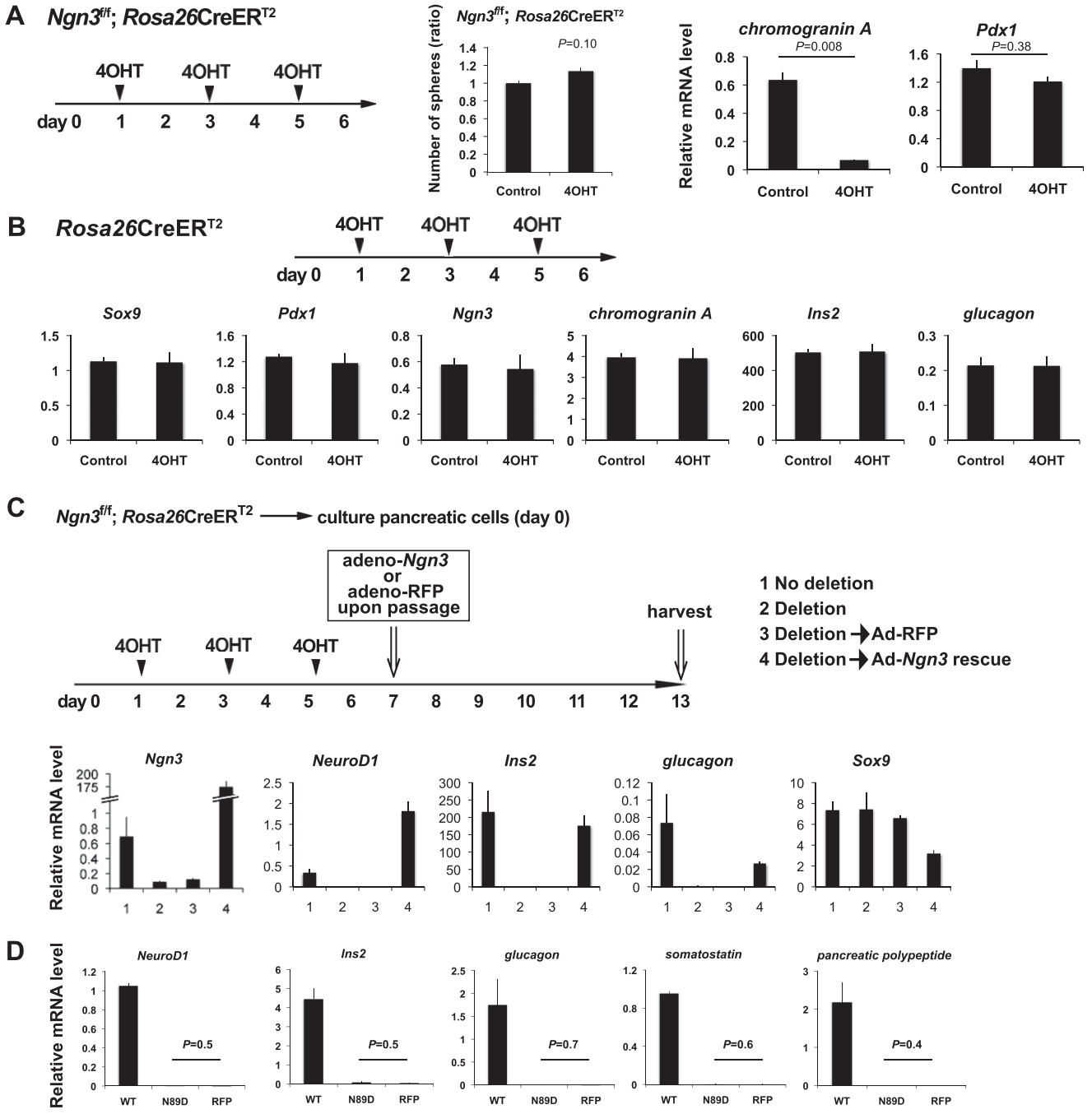

Fig. S7. (*A*) Genetic deletion of *Ngn3* does not affect sphere formation (*Ngn3*$^{f/f}$; *Rosa26*CreER^{T2}: *Middle*). Both the number and the size of the spheres were not significantly affected by the deletion. (*Left*) Schematic summarizing the experimental strategy. (*Right*) Quantitative RT-PCR analysis of *Ngn3* gene deletion experiments (n = 3). (*B*) *Rosa26*CreER^{T2} control spheres do not alter the expression of developmental genes on 4-hydroxytamoxifen treatment. Spheres generated from *Rosa26*CreER^{T2} pancreatic cells were treated with 4-hydroxytamoxifen (*Upper*) and assessed using quantitative RT-PCR analysis to measure expression of the indicated markers (*Lower*). The number and the size of the spheres were not significantly affected by exposure to 4-hydroxytamoxifen (n = 5). (*C* and *D*) Genetic rescue of *Ngn3* deficiency in pancreatic spheres. (*C*; *Upper*) Schematic summarizing the experimental strategy for Cre recombinase-based inactivation of conditional *Ngn3* followed by restoration with adenoviral infection of wild-type mouse *Ngn3* (Ad-*Ngn3*). (*Lower*) Quantitative RT-PCR analysis of *Ngn3* gene deletion rescued by adeno-mouse *Ngn3* (n = 5). (*D*) Quantitative RT-PCR analysis of the designated genes expressed in *Ngn3*-deficient spheres infected with Ad-h*NGN3* (wild-type), Ad-h*NGN3* N89D (a previously reported null allele), or control Ad-RFP (n = 3).

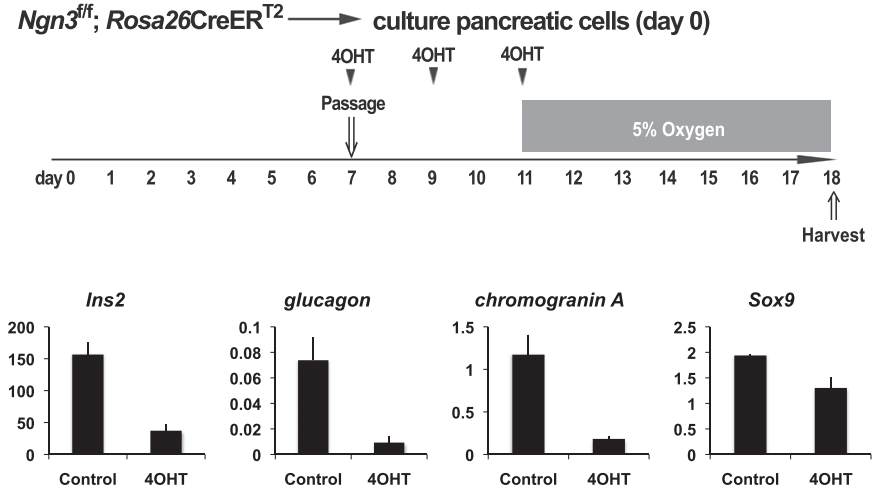

Fig. S8. Oxygen-dependent islet differentiation requires *Ngn3*. (*Upper*) Schematic summarizing the experimental strategy. (*Lower*) Quantitative RT-PCR analysis of the spheres. Compared with controls without deletion of *Ngn3*, deletion of *Ngn3* markedly reduced the expression of pancreatic islet markers *Ins2*, *glucagon*, and *chromogranin A* in physiological oxygen culture. These results are consistent with our interpretation that hormone-negative progenitors are the predominant source of differentiated endocrine cells in sphere culture.

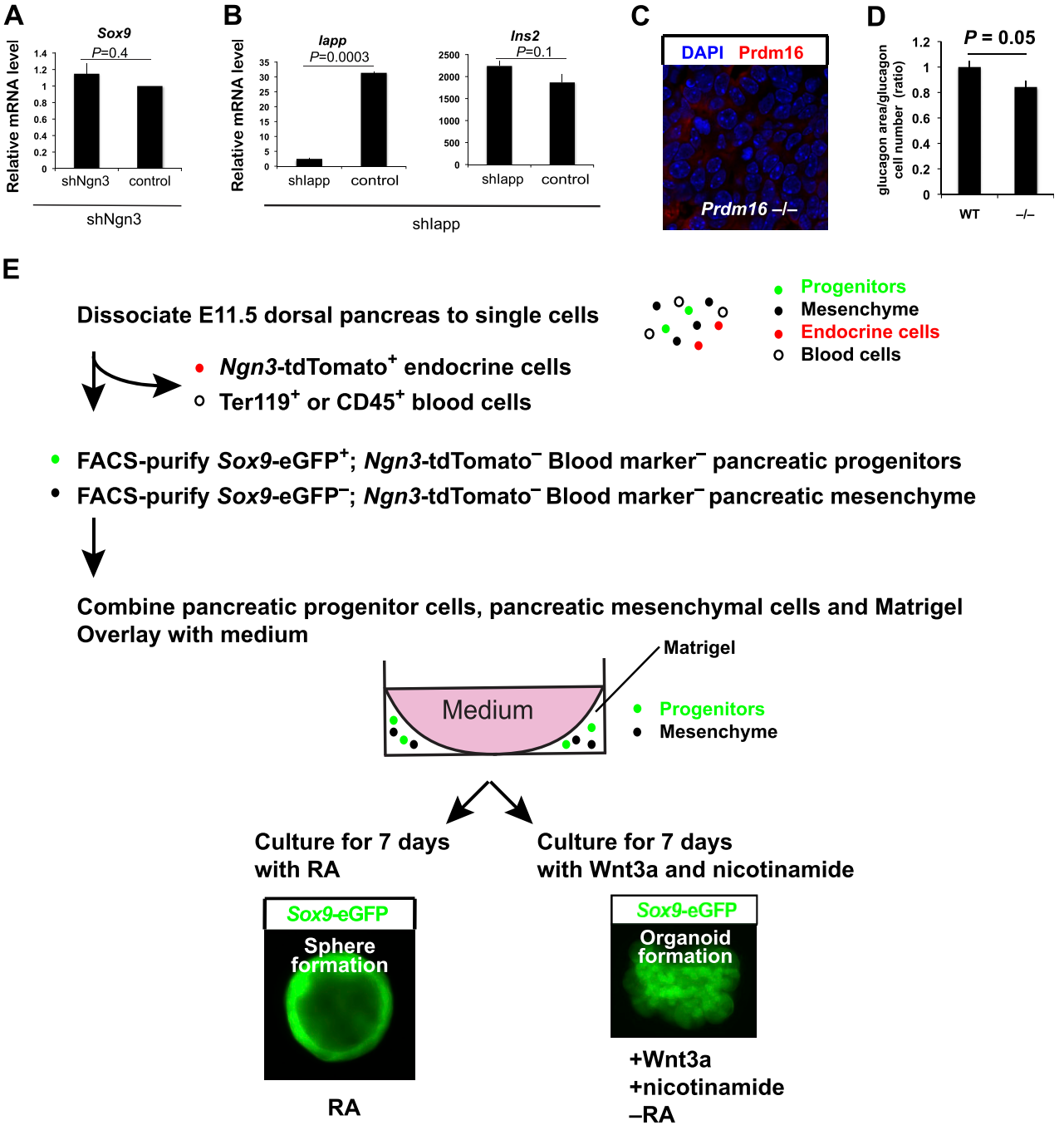

Fig. S9. (*A* and *B*) Functional genetic screening for essential regulators of islet development using sphere assay. (*A*) shRNA-mediated knock-down of *Ngn3* did not change *Sox9* mRNA levels significantly by qRT-PCR ($n = 3$). (*B*) shRNA-mediated knock-down of *Iapp* did not change *Ins2* mRNA levels significantly by qRT-PCR ($n = 3$). (*C*) Prdm16 staining was undetectable in mutant tissues. Confocal images of E15.5 *Prdm16*$^{-/-}$ pancreas. A cryosection was stained with an antibody against Prdm16 (red) and counterstained with DAPI (blue). (*D*) *Prdm16* mutant mice lack detectable α cell hypertrophy. Glucagon area was divided by glucagon cell number to quantify the average α cell size ($n = 3$–4 mice per group). (*E*) Schematic summarizing culture methods generating pancreatic spheres and pancreatic organoids.

Other Supporting Information Files

Dataset S1 (XLS)
Dataset S2 (XLS)
Dataset S3 (XLS)
Dataset S4 (XLS)
Dataset S5 (XLS)